

Genome-Based Discovery of an Unprecedented Cyclization Mode in Fungal Sesterterpenoid Biosynthesis

Masahiro Okada,^{†,‡} Yudai Matsuda,^{†,‡} Takaaki Mitsuhashi,[†] Shotaro Hoshino,[†] Takahiro Mori,[†] Kazuya Nakagawa,[§] Zhiyang Quan,[†] Bin Qin,[†] Huiping Zhang,^{||} Fumiaki Hayashi,^{||} Hiroshi Kawaide,[§] and Ikuro Abe^{*,†}

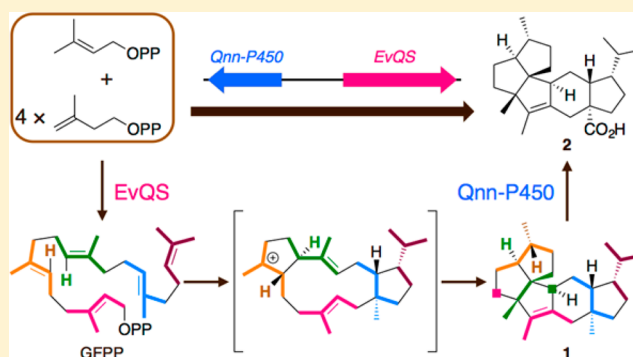
[†]Graduate School of Pharmaceutical Sciences, The University of Tokyo, 7-3-1 Hongo, Bunkyo-ku, Tokyo 113-0033, Japan

[§]Institute of Agriculture, Tokyo University of Agriculture and Technology, 3-5-8 Saiwai-cho, Fuchu, Tokyo 183-8509, Japan

^{||}RIKEN Center for Life Science Technologies, 1-7-22 Suehiro-cho, Tsurumi-ku, Yokohama, Kanagawa 230-0045, Japan

Supporting Information

ABSTRACT: Sesterterpenoids are a group of terpenoid natural products that are primarily biosynthesized via cyclization of the C₂₅ linear substrate geranylgeranyl pyrophosphate (GGPP). Although the long carbon chain of GGPP in theory allows for many different cyclization patterns, sesterterpenoids are relatively rare species among terpenoids, suggesting that many intriguing sesterterpenoid scaffolds have been overlooked. Meanwhile, the recent identification of the first sesterterpene synthase has allowed the discovery of new sesterterpenoids by the genome mining approach. In this study, we characterized the unusual fungal sesterterpene synthase EvQS and successfully obtained the sesterterpene quiannulane (1) with a novel and unique highly congested carbon skeleton, which is further oxidized to quiannulic acid (2) by the cytochrome P450 Qnn-P450. A mechanistic study of its cyclization from GGPP indicated that the biosynthesis employs an unprecedented cyclization mode, which involves three rounds of hydride shifts and two successive C–C bond migrations to construct the 5-6-5-5-5 fused ring system of 1.



INTRODUCTION

Terpenoids are natural products derived from C₅ isoprene units and include numerous compounds with diverse backbone skeletons as well as pharmaceutically important compounds.¹ The complex scaffolds of terpenoids are synthesized via cyclization of the linear, achiral polyisoprenoid substrates, which is initiated by the formation of a carbocationic species. Cyclization events are generally the first committed step in terpenoid biosyntheses and yield terpene hydrocarbons or alcohols. The reactions are catalyzed by terpene cyclases (TCs) and have been of great interest to chemists since a molecular architecture with multiple rings and chiral centers can be constructed in a single reaction (or a few reactions). Hence, a considerable number of TCs have been discovered and characterized enzymologically and structurally, to understand the molecular mechanisms responsible for the diversity generation in terpenoid biosynthesis.^{2–7} However, we are far from the point where we can design an enzyme that achieves a desired cyclization scheme.

Terpenoids are further classified into several subgroups, according to the number of isoprene units utilized in their biosynthesis. Interestingly, sesterterpenoids, which are derived from five C₅ units (or geranylgeranyl pyrophosphate, GGPP), are relatively rare among terpenoid natural products;⁸ C₁₅

sesquiterpenoids, C₂₀ diterpenoids, and C₃₀ triterpenoids are more common than C₂₅ sesterterpenoids. Accordingly, much less is known about the enzymes involved in sesterterpenoid biosynthesis, as compared to those for the other classes of terpenoids. However, given that a longer substrate should contribute to greater product diversity, the chemical space of sesterterpenoids could be much larger than what we currently recognize. Therefore, it is likely that we have overlooked numerous sesterterpenoids and we may even be able to induce novel cyclization modes of GGPP by the engineering of TCs. Thus, mining for largely undiscovered sesterterpenoids and their synthases could provide molecules with novel scaffolds as well as insights into the enzymatic processes that afford their carbon skeletons.

The first sesterterpene synthase identified was ophiobolin F synthase (AcOS) from the fungus *Aspergillus clavatus*,⁹ which led to the discovery of several new sesterterpenes by searching for and characterizing genes homologous to AcOS in fungal genomes.^{10–13} These enzymes are chimeric proteins consisting of two domains: a prenyltransferase (PT) domain at the C-terminus and a TC domain at the N-terminus. Thus, it appears

Received: June 6, 2016

Published: July 22, 2016

that the GFPP produced by the PT is efficiently transferred to the TC to yield a cyclized product. Intriguingly, a recent phylogenetic analysis of the TCs of these bifunctional terpene synthases suggested that the enzymes could be grouped into five clades (clades A–E), with TCs in the same clade performing the same initial cyclization of the substrate.¹¹ So far, this hypothesis is consistent with reactions by the known fungal sesterterpene synthases (and homologous diterpene synthases^{14–16}) but is supported by only a limited number of characterized enzymes. Thus, it is important to expand our knowledge of this class of enzymes, since this information would contribute to obtaining new natural products and provide opportunities to artificially modify the functions of TCs. In this study, we focused on the sesterterpene synthase EvQS, a TC that is not grouped into any previously proposed clade, and demonstrated that EvQS is responsible for the formation of a pentacyclic sesterterpene quiannulatene (**1**) with an unprecedented carbon skeleton (Figure 1). We also

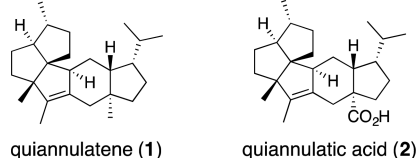


Figure 1. Sesterterpenoids obtained in this study.

elucidated the mechanism that affords the unique pentacyclic scaffold of **1** by in vivo isotope incorporation using labeled acetates and by in vitro experiments with GFPP isotopomers generated in situ. Finally, we found that **1** is further transformed into its carboxylate derivative, quiannulatic acid (**2**), by the cytochrome P450 monooxygenase encoded by the gene located next to EvQS. Sequence data for the biosynthetic gene cluster for quiannulatic acid have been deposited at DDBJ/EMBL/GenBank under Accession Number LC155210.

RESULTS AND DISCUSSION

Search for a Sesterterpene Synthase Gene and Its Functional Analysis. To obtain a new metabolite derived from a fungal bifunctional terpene synthase, we focused on *Emericella varicolor* NBRC 32302 as a potential source, since we previously identified several new sesterterpenes from this fungus and its genome encodes many yet-uncharacterized putative sesterterpene synthases.^{10,12,13} Among these candidates, one gene encoding a protein with 746 amino acid residues was selected (Figure S1), since its TC domain belongs to none of the clades A–E (Figure S2). Therefore, we expected that a novel terpene molecule, generated via a different initial cyclization mode from the previously characterized modes, could be obtained. To analyze the function of this gene, it was heterologously expressed in *Aspergillus oryzae* NSAR1,¹⁷ as this strain is suitable for the characterization of fungal biosynthetic enzymes.^{18,19} The transformant was cultivated in the induction medium, and the resulting mycelial metabolites were analyzed by gas chromatography–mass spectrometry (GC-MS). As a result, we detected the new metabolite **1** with m/z 340 $[M]^+$ (Figure 2A and Figure S3A), which corresponds to the molecular weight of a sesterterpene hydrocarbon. The GC retention time and the mass spectrum of **1** indicated that **1** is not identical to the other terpene compounds obtained in our

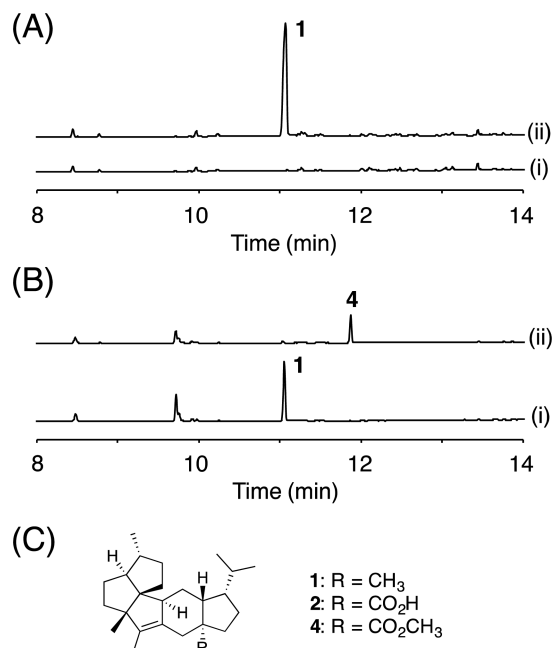


Figure 2. Functional analyses of EvQS and Qnn-P450. (A) GC-MS chromatograms of mycelial extracts from *A. oryzae* transformants harboring (i) only empty vector or (ii) EvQS. (B) GC-MS chromatograms of mycelial extracts methylated by (trimethylsilyl)-diazomethane from *A. oryzae* transformants harboring (i) EvQS or (ii) EvQS and Qnn-P450. (C) Structures of **1**, **2**, and **4**.

previous studies,^{10,12,13} and thus it was isolated for structural characterization.

High-resolution electron ionization mass spectrometric (HR-EI-MS) analysis revealed the molecular formula of **1** as $C_{25}H_{40}$ with six degrees of unsaturation. In the ^{13}C NMR spectrum of **1**, 25 signals, including two olefinic carbons, were accordingly observed, suggesting the pentacyclic backbone of **1**. Further interpretation of the two-dimensional NMR spectra successfully established the planar structure of **1**, with an unprecedented molecular architecture (Figure 3A, Table S3, and Figures S10–

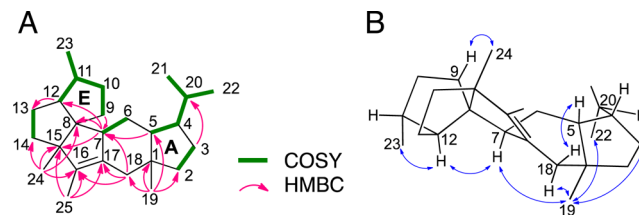


Figure 3. (A) 1H – 1H correlation spectroscopy (COSY) and key heteronuclear multiple-bond correlation (HMBC) correlations in **1**. (B) Key NOESY correlations in **1**.

S17; see Supporting Information for details of structural determination). The relative configuration of **1** was then determined, based on the nuclear Overhauser effect spectroscopic (NOESY) correlations (Figure 3B). For the stereochemistry of the A and B rings, the $1S^*,4S^*,5R^*,7S^*$ configuration was deduced on the basis of correlations of H-19 with H-7/H-18 α /H-20/H-22 and H-5 with H-18 β . Subsequently, the $8R^*,11R^*,12S^*,15R^*$ configuration for the C, D, and E rings was established by correlations of H-7 with H-12, H-9 with H-24, and H-12 with H-23. Thus, we

determined that **1** has a novel scaffold with a 5-6-5-5-5 fused ring system, including an intriguing angular triquinane moiety.

We then aimed to establish the absolute configuration of **1**, but the unfunctionalized nature of **1** prevented the rapid determination of its complete structure. We therefore sought to synthetically derivatize **1** to a compound to which a known methodology for absolute configuration determination could be applied. After investigation of several oxidative reactions of **1**, selenium dioxide oxidation was found to efficiently convert **1** into the conjugated aldehyde **3** (Figure 4, Table S5, and Figures

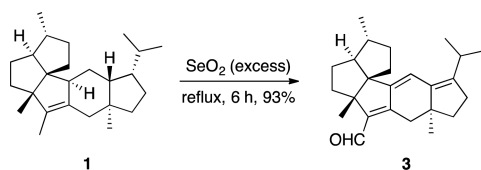


Figure 4. Derivatization of **1** by oxidation with selenium dioxide.

S26–S33). The electron circular dichroic (ECD) spectrum of **3** in ethanol was then compared with the calculated ECD data of **3**, and thus we established the absolute configuration of **1** to be 1*S*,4*S*,5*R*,7*S*,8*R*,11*R*,12*S*,15*R* (Tables S8–S11 and Figures S5–S9). The sesterterpene **1** was hereby named quiannulatene, and the sesterterpene synthase was designated as EvQS (*E. varicolor* quiannulatene synthase).

Functional Analysis of the Cytochrome P450 That Oxidizes 1. Since the metabolites produced by terpene synthases are often further transformed into their derivatives in many biosynthetic pathways, we then investigated whether quiannulatene (**1**) could be converted to a new compound by tailoring enzyme(s). To this end, we investigated the flanking regions of EvQS, and found a gene encoding a putative cytochrome P450 monooxygenase located next to the EvQS gene. On the basis of the fact that P450s are commonly involved in fungal sesterterpenoid biosynthesis and that they are often responsible for the oxidation of a methyl group into a carboxylate,^{10,11} we reasoned that Qnn-P450 is engaged in the transformation of **1** into its carboxylate counterpart.

To illuminate the function of Qnn-P450, the P450 gene was coexpressed with EvQS in *A. oryzae*, and the resultant metabolites were subsequently methylated with (trimethylsilyl)diazomethane prior to GC-MS analysis, to detect molecules with a carboxylate functionality. A new compound, **4**, with m/z 384 $[M]^+$, which corresponds to the molecular weight of the methyl ester of a sesterterpene monocarboxylate, was detected only in the extract from the transformant expressing both genes (Figure 2B and Figure S3E). The new metabolite **2**, whose methylation gives **4**, was isolated and analyzed by NMR. The NMR spectra of **2** were highly similar to those of **1** but revealed the disappearance of one singlet signal for a methyl group in the ¹H NMR spectrum, as well as the presence of a new signal for a carboxylic acid (δ 184.0) in the ¹³C NMR spectrum, indicating that **2** is a derivative of **1** with a carboxyl group. Two-dimensional (2D) NMR spectra of **2** confirmed that a carboxyl functionality was introduced to the C-19 methyl group (Figure 2C, Table S4, and Figures S18–S25), and we deduced that **2** has the same configuration as that of **1**, which established the structure of **2**. Collectively, Qnn-P450 oxidizes C-19 of **1** in three successive reactions to afford the carboxylate **2**, which was accordingly named quiannulatide acid.

P450s are often encoded by genes in the biosynthetic gene clusters for fungal sesterterpenoids, and they are responsible for multistep oxidative reactions. The carboxylation of a methyl group is a typical tailoring reaction by a P450, but a recent study revealed that a P450 can perform much more complex reactions on a sesterterpene scaffold, such as heterocyclization.²⁰ These P450s, as well as many uncharacterized ones found in fungal genomes, may possess cross-reactivities on other sesterterpene species than their own substrates, and thus they could be used as tools to derivatize sesterterpene skeletons in unnatural manners. Finally, we also investigated whether the new compounds **1–3** exhibit some biological activities, but unfortunately, they displayed neither antimicrobial activity nor cytotoxicity.

Mechanism of Cyclization Catalyzed by EvQS. To obtain insight into how EvQS yields the highly congested, unique backbone of quiannulatene (**1**), the cyclization mechanism to afford **1** was investigated through several isotope-labeling experiments. Initially, the transformant harboring EvQS was incubated in the presence of sodium $[1-^{13}\text{C}]$ -acetate, to clarify the distribution of the five isoprene units used to synthesize **1**. As fungi employ the mevalonate pathway, we used dimethylallyl pyrophosphate (DMAPP) and isopentenyl pyrophosphate (IPP) labeled with ¹³C at positions C-1 and C-3 as substrates, thus providing GFPP labeled at 10 positions (Figure 5A). Accordingly, **1** was labeled with ¹³C at ten distinct positions: C-1, -3, -6, -9, -11, -13, -15, -16, -18, and -19 (Figure 5A and Figure S34). The labeling pattern, however, did not provide an unambiguous conclusion about how GFPP is folded to generate the carbon skeleton of **1**.

To overcome this problem, we then performed in vitro labeling experiments with enzymatically prepared GFPP isotopomers. For this purpose, we first sought to express EvQS in *Escherichia coli*, but we were not able to obtain a soluble enzyme when the intact gene was expressed. Therefore, we prepared a truncated EvQS protein containing only the TC domain. The in vitro enzymatic reaction with the TC of EvQS and the PT domain of another terpene synthase, EvVS,¹² successfully produced **1** from IPP and DMAPP as substrates (Figure S4A), thus confirming the activities of the two enzymes. We previously developed an “enzyme cocktail” that enables the in vitro synthesis of (poly)prenylpyrophosphates from acetate or mevalonate as a starting material, which has been successfully applied to the enzymatic total synthesis of several terpenes and terpenoids.^{21–23} Utilizing the enzyme cocktail, we prepared $[U-^{13}\text{C}_5]$ IPP from $[U-^{13}\text{C}_6]$ mevalonate, which was ligated with unlabeled geranylgeranyl pyrophosphate (GGPP) by the PT of EvVS to yield $[1,2,3,4,20-^{13}\text{C}_5]$ GFPP, possessing the ¹³C label on the first isoprene unit at the tail. Cyclization of this labeled GFPP by the TC of EvQS synthesized **1**, possessing ¹³C at the C-14, -16, -17, -18, and -25 positions (Figure 5C and Figures S3C and S35). Similarly, two molecules of $[U-^{13}\text{C}_5]$ IPP were ligated with unlabeled farnesyl pyrophosphate (FPP) to afford $[1,2,3,4,5,6,7,8,20,21-^{13}\text{C}_{10}]$ GFPP, the cyclization of which gave a product with five additional ¹³C labels at the C-10, -11, -12, -13, and -23 positions (Figure 5C and Figures S3D and S36). Taken together, the distribution of each isoprene unit of GFPP in the structure of **1** can now be well predicted (Figure 5D).

We then focused on the origin of each hydrogen atom in **1**. Initially, the enzymatic reaction was performed in the presence of ²H₂O on the basis of our previous report,¹³ since several studies demonstrated that ²H₂O can be utilized to probe the

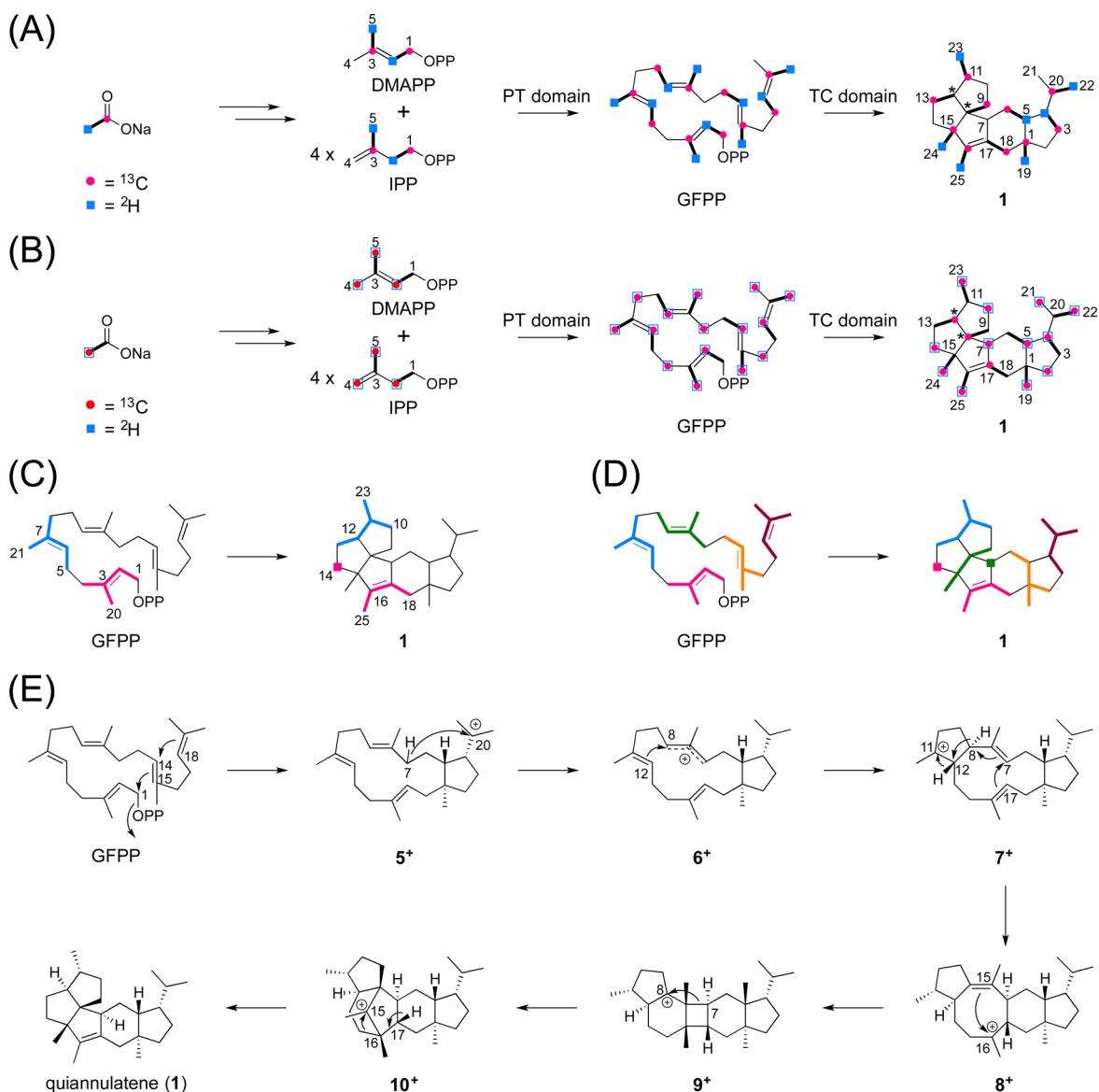


Figure 5. Summary of labeling experiments of **1** using (A) sodium $[1\text{-}^{13}\text{C}]/[1\text{-}^{13}\text{C}, 2\text{H}_3]$ acetate or (B) sodium $[2\text{-}^{13}\text{C}, 2\text{H}_3]$ acetate. Bold lines indicate acetate units. Asterisks indicate carbons from which the deuterium label was lost. (C) Experimentally confirmed distribution of carbons derived from the first two isoprene units at the tail of GFPP. (D) Deduced distribution of all isoprene units in the structure of **1**. (E) Proposed reaction mechanism for generation of **1**.

occurrence of the reprotonation step during the cyclization.^{24–29} As a result, incorporation of a deuterium to **1** was not observed (Figures S3B and S4B), indicating that **1** is produced by a single reaction from GFPP. Furthermore, we incorporated sodium $[1\text{-}^{13}\text{C}, 2\text{H}_3]$ acetate or sodium $[2\text{-}^{13}\text{C}, 2\text{H}_3]$ acetate into **1**, using the *A. oryzae* transformant expressing *EvQS*. The resultant labeling patterns indicated that the deuterium atoms originally bound to C-8 and C-12 were lost from these positions and were transferred to C-12 and C-11, respectively, by 1,2-hydride shifts (Figure 5A, B, Figures S37 and S38, and Tables S6 and S7; see Supporting Information for detailed interpretation of the NMR spectra).

With all the experimental data described above, a plausible mechanism for the *EvQS*-catalyzed cyclization can be proposed as follows (Figure 5E). The initial cyclizations following elimination of the pyrophosphate group of GFPP occur at C-1/C-15 and C-14/C-18, to yield 5^+ with the 15-5 fused ring system. A 1,5-hydride shift between C-7 and C-20 would

provide 6^+ , in which the carbocation is stabilized by delocalization. Although there are other possibilities for neutralization of the C-20 cation (e.g., a series of 1,2-hydride shifts or two rounds of 1,3-hydride shifts), the one-step hydride shift would be most likely for this event, since a similar 1,5-hydride shift was proposed and experimentally proved in the cyclization reaction leading to sesterfisherol.¹¹ The C–C bond at C-8/C-12 would then be formed to give the tricyclic species 7^+ , which undergoes two rounds of 1,2-hydride shifts (C-12 to C-11 and C-8 to C-12) followed by the double-bond isomerization and C–C bond formation at C-7/C-17 to yield 8^+ . Subsequently, the π electrons of the double bond attack the carbocation at C-16 to afford the 5-6-4-6-5 fused pentacyclic carbocationic species 9^+ , and the alkyl shift would newly create the C–C bond at C-7/C-8 to provide 10^+ . Finally, the alkyl shift from C-16 to C-15, followed by deprotonation from C-17, would afford the pentacyclic backbone of **1** and install the

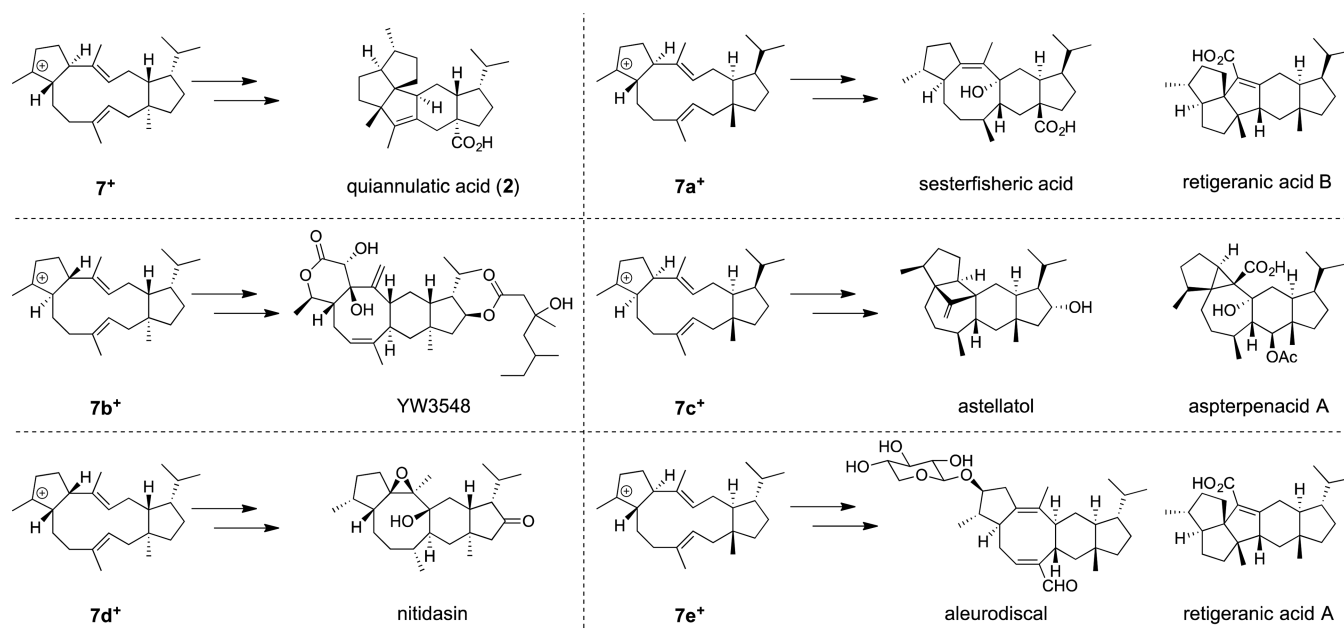


Figure 6. Series of diastereomeric tricyclic cationic species in GFPP cyclization events (7^+ and $7a^+–7e^+$) and selected fungal sesterterpenoids probably derived from these diastereomers.

double bond between C-16 and C-17, completing the cyclization cascade.

The proposed mechanism resembles that for sesterfisherol, especially in the first halves of their reactions, despite the low sequence identity between EvQS and sesterfisherol synthase (~20% identity in their TC domains).¹¹ Importantly, the stereochemistry of 5^+ , deduced from the structure of **1**, is not the same as that proposed for the intermediate of sesterfisherol; they are enantiomers of each other. Thus, EvQS adopts a different initial cyclization pattern from that of any other previously characterized fungal bifunctional terpene synthase, which might explain why the TC of EvQS belongs to none of the clades A–E. Furthermore, the diastereomers of 7^+ are proposed to widely serve as key intermediates in cyclization events for sesterterpenoid generation, such as retigeranic acids A and B,^{30,31} YW3548,³² astellatol,³³ aspterpenacid A,³⁴ nitidasin,³⁵ and aleurodiscal,³⁶ and five diastereomers ($7a^+–7e^+$) have been proposed to be utilized in the synthesis of sesterterpenoids¹¹ (Figure 6). Intriguingly, to the best of our knowledge, no sesterterpenoids known to date appear to be derived from 7^+ , thus suggesting the presence of a new member for the diastereomer series of 7^+ in terpenoid biosynthesis.

Genome mining of fungal sesterterpene synthases has been proved to be a powerful tool to obtain new terpenoids with novel scaffolds, but BLAST searches using these enzymes as queries suggest that a number of uncultivated possible sesterterpene synthases still remain. For example, proteins sharing relatively high sequence identity (40–50%) with the TC of EvQS can be found in publicly available databases, although EvQS belongs to a new clade, which we now call clade F. Given that these homologues are encoded by fungi in different families and that the mining for sesterterpene synthases has only been performed against fungi in the family Trichocomaceae, it would be important to focus on the enzymes derived from a variety of fungi to further expand the molecular diversity of sesterterpenoids.

CONCLUSION

Since the first discovery of a sesterterpene synthase in 2013, several new sesterterpenes (or sesterterpenoids) have been successfully isolated by genome mining and heterologous expression approaches. In this study, we sought to obtain a sesterterpene with a novel scaffold by focusing on an enzyme that is less similar to the previously characterized ones, and we successfully identified and characterized the bifunctional sesterterpene synthase EvQS, which produces quiannulatene (**1**) with a unique, highly congested carbon skeleton. Additionally, *in vivo* and *in vitro* isotope labeling experiments with different substrates provided clear evidence for the occurrence of hydride shifts and C–C bond migrations in the cyclization scheme, and thus allowed the proposal of a plausible mechanism for the generation of **1**. Importantly, the early-stage cyclization mode of GFPP to afford **1** does not appear to be utilized in the biosyntheses of any other known sesterterpenoids, suggesting that the functional analyses of terpene cyclases belonging to the same clade as EvQS could lead to the discovery of other novel terpene backbone structures. To shed further light on structural details of the enzyme reactions, crystallization and structure–function studies of these chimeric enzymes are in progress. In conclusion, the genome-based approach to the search for sesterterpenoids would definitely contribute to the isolation of many overlooked terpene species and expand the chemical space of natural products.

MATERIALS AND METHODS

Strains and Media. *Emericella variegata* NBRC 32302 was obtained from the Biological Resource Center, National Institute of Technology and Evaluation (Chiba, Japan). *E. variegata* NBRC 32302 was cultivated at 30 °C and 160 rpm in DPY medium [2% dextrin, 1% hipolypepton (Nihon Pharmaceutical Co., Ltd.), 0.5% yeast extract (Difco), 0.5% KH_2PO_4 , and 0.05% $\text{MgSO}_4 \cdot 7\text{H}_2\text{O}$] for 3 days and used as a source for cloning of the EvQS and Qnn-P450 genes. For the extraction of RNA, the strain was statically cultivated at 28 °C in malt extract broth [2% malt extract (Difco), containing 2% glucose and 0.1% mycological peptone (Oxoid)] for 3 weeks.

Aspergillus oryzae NSAR1 (*niaD*⁻ *sC*⁻ Δ *argB* *adeA*⁻)¹⁷ was used as the host for fungal expression. Transformants of the *A. oryzae* strain were grown in shaking cultures in DPY medium at 30 °C and 160 rpm for 5 days.

Standard DNA engineering experiments were performed with *Escherichia coli* DH5 α , purchased from Clontech (Mountain View, CA). *E. coli* cells carrying each plasmid were grown in Luria–Bertani (LB) medium and were selected with appropriate antibiotics. *E. coli* Rosetta 2 (DE3) codon plus (Novagen) was used for expression of the TC domain of EvQS and the PT domain of EvVS.

Phylogenetic Analysis. The phylogenetic tree of the TC domains of fungal chimeric terpene synthases was drawn by use of CLC Sequence Viewer 7.7 (CLC bio) with the Jukes–Cantor distances analysis (UPGMA algorithm).

Construction of Fungal Expression Plasmids and Transformation of *A. oryzae* NSAR1. For construction of fungal expression plasmids, each gene was amplified from *E. varicolor* NBRC 32302 genomic DNA, with the primers listed in Tables S1 and S2. The full-length genes were purified, digested with appropriate restriction enzymes, and ligated into the pTAex3³⁷ vector by use of a ligation kit v2.1 (TaKaRa) according to the manufacturer's protocol (Table S2). For introduction of the *Qnn-P450* gene into pAdeA,³⁸ a fragment containing the *amyB* promoter (*PamyB*) and the *amyB* terminator (*TamyB*) was amplified from the pTAex3-based plasmid and ligated into pAdeA (Table S2).

Transformation of *A. oryzae* NSAR1 was performed by the protoplast–poly(ethylene glycol) method, as reported previously.³⁹ To coexpress EvQS and *Qnn-P450*, two plasmids, pTAex3-EvQS and pAdeA-*Qnn-P450*, were used for transformation. For construction of negative control strains, the corresponding void vectors were used for transformation.

Gas Chromatographic–Mass Spectrometric Analysis of Each Metabolite. For analysis of the mycelial extract from the *A. oryzae* transformant harboring EvQS, the extract was subjected to GC-MS analysis. The temperature of the ionization chamber was 280 °C, with electron impact ionization at 70 eV. Helium was used as a carrier gas, and its linear velocity was 44.9 cm/min. The program held the temperature at 150 °C for 4 min, increased the temperature at a rate of 15 °C/min up to 330 °C, and then held it at 330 °C for 10 min.

For analysis of the mycelial extract from the *A. oryzae* transformant harboring EvQS and *Qnn-P450*, the extract was methylated with (trimethylsilyl) diazomethane prior to GC-MS analysis, by adding 50 μ L of a 0.6 M hexane solution to the extract, dissolved in 100 μ L of benzene and 100 μ L of methanol, and incubating the mixture at room temperature for 1 h. GC-MS conditions were the same as those described above for the EvQS product.

Isolation and Purification of Each Metabolite. For purification of quiannulatene (**1**), mycelia from 2 L of a culture of the *A. oryzae* transformant with the EvQS gene were extracted with acetone at room temperature overnight. The extract was concentrated, reextracted with hexane, and then subjected to silica gel column chromatography with elution by hexane, yielding 18 mg of a colorless oil.

For purification of quiannulatic acid (**2**), mycelia from 2 L of a culture of the *A. oryzae* transformant with the EvQS and *Qnn-P450* genes were extracted with acetone at room temperature overnight. The extract was concentrated, reextracted with ethyl acetate, and then subjected to silica gel column chromatography, in which the silica gel was pretreated with oxalic acid, with elution by a hexane/ethyl acetate gradient (100/0 to 84/16). The fractions that contained **2** were further purified by reverse-phase preparative HPLC (95% aqueous acetonitrile with 0.5% acetic acid, 3.0 mL/min) to yield 9.0 mg of a colorless oil.

Synthesis of **3.** To a solution of **1** (7.00 mg, 20.6 μ mol) in anhydrous CH₂Cl₂ (5.5 mL) was added an excess amount of selenium dioxide (25.0 mg, 225 μ mol), and the mixture was stirred for 3 h at reflux. Subsequently, additional selenium dioxide (28.0 mg, 252 μ mol, suspended in 3 mL of CH₂Cl₂) was supplied to the reaction mixture, and it was stirred for another 3 h at reflux. After the CH₂Cl₂-insoluble matter was removed by decantation, the reaction mixture was concentrated by evaporation. The resulting residue was subjected to

flash silica gel column chromatography (hexane/ethyl acetate = 100/0 to 95/5) to give **3** as a yellowish oil (6.70 mg, 19.1 μ mol, 93%).

Electron Circular Dichroism Calculation. All theoretical calculations of **3** were performed with Gaussian 09.⁴⁰ Conformational analysis of **3** was initially performed with the ChemBio3D Ultra 14.0 software, using the Merck molecular force field 94x (MMFF94x),⁴¹ and four conformers (**3a–3d**) were obtained with an energy cutoff of 15 kJ/mol. These conformers were then further optimized by use of density functional theory (DFT) at the B3LYP/6-31G(d) level, with a polarizable continuum model (PCM) in ethanol. Frequency calculations were used to check that each conformer has the minimum energy. From the distribution of each optimized conformer, based on their thermodynamic parameters and the Boltzmann distribution law at 298 K, two major conformers (**3a** and **3b**) were selected for ECD calculations. ECD calculations of **3a** and **3b** were performed by time-dependent density-functional theory (TD-DFT) at the B3LYP/6-31+(d,p) level, with a PCM in ethanol. Finally, the calculated ECD curves of **3a** and **3b** were weighted by the Boltzmann law, and the resulting spectra were compared with the experimentally obtained spectra (Tables S8–S11 and Figures S5–S9).

In Vivo Labeling Experiments of **1.** For labeling experiments with sodium [1-¹³C]acetate, an *A. oryzae* transformant harboring the EvQS gene was cultivated in 200 mL of DPY medium supplemented with 0.01% adenine and 100 mg of the labeled acetate, at 30 °C and 160 rpm for 5 days. When sodium [1-¹³C,²H₃]acetate or sodium [2-¹³C,²H₃]acetate was used, the transformant was cultivated in 250 mL of DPY medium supplemented with 20 mg of the labeled acetate, at 30 °C and 160 rpm for 3 days. Mycelia from each transformant were extracted with acetone at room temperature overnight. The extracts were concentrated, reextracted with hexane, and subjected to silica gel column chromatography with elution by hexane, to yield 2.6 mg, 2.0 mg, and 2.1 mg of colorless oil from sodium [1-¹³C]acetate, sodium [1-¹³C,²H₃]acetate, and sodium [2-¹³C,²H₃]acetate, respectively. The labeled quiannulatene (**1**) was then subjected to ¹³C NMR analyses (Tables S6 and S7 and Figures S34, S37, and S38).

Expression, Purification, and Reaction of Recombinant Proteins. To remove the fusion tag from the pCold-TF vector, the region except for the tag was amplified by use of primers pCold-F and pCold-R (Table S1). This vector was designated as pColdX. To obtain intron-free genes, total RNA was extracted from *E. varicolor* NBRC 32302 by use of Isogen (Nippon Gene Co., Ltd.), and cDNA was synthesized with SuperScript III reverse transcriptase (Invitrogen) from the extracted RNA. The PT domain of EvVS, [356–705]EvVS, and the TC domain of EvQS, [1–381]EvQS, were amplified and cloned into the pCold-TF vector and the pColdX vector, respectively, by use of the primers and conditions shown in Tables S1 and S2. *E. coli* Rosetta 2 (DE3) codon plus cells harboring each plasmid were cultured to an OD₆₀₀ of 0.5 in LB medium containing 100 mg/L ampicillin at 37 °C. Isopropyl β -D-1-thiogalactopyranoside was then added to a final concentration of 0.50 mM to induce gene expression, and the cultures were incubated further for 18 h at 15 °C. *E. coli* cells were harvested by centrifugation at 5800g and resuspended in 50 mM Tris-HCl buffer (pH 8.4) containing 250 mM NaCl, 10% (v/v) glycerol, 5 mM MgCl₂, and 5 mM imidazole (buffer A). The cells were disrupted by sonication, and the lysate was centrifuged at 7300g for 30 min. The supernatant was loaded onto a Cosmogel His-Accept (Nacalai Tesque) column equilibrated with buffer A. After the resin was washed with buffer A containing 10 mM imidazole, the recombinant proteins were subsequently eluted with buffer A containing 300 mM imidazole. Protein solution buffers were substituted with 50 mM Tris-HCl buffer (pH 8.4) containing 250 mM NaCl, 10% (v/v) glycerol, and 5 mM MgCl₂. All purification procedures were performed at 4 °C.

The standard enzymatic reaction was performed in mixtures containing 100 mM Tris-HCl (pH 7.5), 10 μ g of DMAPP, 10 μ g of IPP, 5 mM MgCl₂, 100 μ g of [1–381]EvQS, and 200 μ g of [356–705]EvVS in a final volume of 450 μ L. After incubation at 30 °C overnight, the reaction was extracted with 250 μ L of ethyl acetate three times and analyzed by GC-MS. The temperature of the ionization chamber was 250 °C, with electron impact ionization at 70 eV. Helium

was used as a carrier gas, and its linear velocity was 44.9 cm/min. The program maintained the temperature at 100 °C for 3 min, increased the temperature at a rate of 14 °C/min up to 268 °C, and then held it at 268 °C for 4 min.

Preparation and Reactions of GFPP Isotopomers. The $[U-^{13}C_5]$ IPP reaction mixture was prepared by an incubation of 1.8 mM $[U-^{13}C_6]$ MVA with three enzymes and cofactors, including mevalonate kinase (40 g/L), phosphomevalonate kinase (40 g/L), and diphosphomevalonate decarboxylase (40 g/L), in 50 mM Tris-HCl buffer (pH 7.5) containing 16 mM ATP and 20 mM $MgCl_2$ at 30 °C for 16 h. The reaction was stopped by heating at 65 °C for 5 min, and the labeled IPP was retrieved from the protein debris by centrifugation at 20900g for 10 min at 4 °C. The enzymes for the IPP synthesis were prepared as previously described.²²

Synthesis of $[14,16,17,18,25-^{13}C_5]$ -1 from $[1,2,3,4,20-^{13}C_5]$ GFPP was performed by incubation of natural-abundance GGPP (0.9 mg) and an excess amount of $[U-^{13}C]$ IPP in a reaction mixture with truncated $[356-705]$ EvVS (10.7 mg) and $[1-381]$ EvQS (5.0 mg) at 30 °C for 12 h. The enzyme product was extracted with hexane and was subjected to ^{13}C NMR analysis without further purification. Similarly, $[10,11,12,13,14,16,17,18,23,25-^{13}C_{10}]$ -1 was synthesized by incubation of natural-abundance FPP (1.0 mg) and an excess amount of $[U-^{13}C]$ IPP in a reaction mixture with truncated $[356-705]$ EvVS (10.0 mg) and $[1-381]$ EvQS (5.0 mg). The enzyme product was partially purified by silica gel column chromatography, with elution by hexane, and was subjected to ^{13}C NMR analysis.

Analytical Data. *Quiannulatene* (1). Colorless oil; $[\alpha]_D^{28}$ 41.7 (c 1.333, C_6D_6); for 1H and ^{13}C NMR data, see Table S3 and Figures S10–S17; HR-EI-MS found m/z 340.3131 $[M]^+$ (calcd 340.3130 for $C_{25}H_{40}$).

Quiannulatic Acid (2). Colorless oil; $[\alpha]_D^{28}$ 123.7 (c 0.033, C_6D_6); for 1H and ^{13}C NMR data, see Table S4 and Figures S18–S25; HR-EI-MS found m/z 370.2885 $[M]^+$ (calcd 370.2872 for $C_{25}H_{38}O_2$).

Compound 3. Yellowish oil; $[\alpha]_D^{25} = -79.7$ (c 0.123, $CHCl_3$); CD (c 0.5, EtOH) $[\theta]_{405} = -20\ 900$, $[\theta]_{345} = +10\ 400$, $[\theta]_{289} = +3600$, $[\theta]_{233} = -12\ 700$; for 1H and ^{13}C NMR data, see Table S5 and Figures S26–S33; HR-MALDI-MS m/z 351.2692 $[M + H]^+$ (calcd 351.2688 for $C_{25}H_{35}O$).

■ ASSOCIATED CONTENT

● Supporting Information

The Supporting Information is available free of charge on the ACS Publications website at DOI: 10.1021/jacs.6b05799.

Additional text with experimental details; 11 tables listing primers, plasmids, NMR data for 1–3, and thermodynamic parameters, conformational analysis, and excited states for conformers of 3; 38 figures showing sequence alignment, phylogenetic analysis, mass spectra, GC-MS profiles, ECD spectra, optimized geometries, molecular orbitals, and 1H NMR, ^{13}C NMR, DEPT-135, DQF-COSY, HSQC, HMBC, and NOESY spectra of 1–3 (PDF)

■ AUTHOR INFORMATION

Corresponding Author

*abei@mol.f.u-tokyo.ac.jp

Author Contributions

[‡]M.O. and Y.M. contributed equally.

Notes

The authors declare no competing financial interest.

■ ACKNOWLEDGMENTS

We thank Professor K. Gomi (Tohoku University) and Professor K. Kitamoto (The University of Tokyo) for kindly providing the expression vectors and the fungal strain. We

thank Professor H. Oikawa (Hokkaido University) and Professor T. Kuzuyama (The University of Tokyo) for kindly providing labeled materials and helpful discussions. This work was supported by Grants-in-Aid for Scientific Research from the Ministry of Education, Culture, Sports, Science and Technology, Japan (JSPS KAKENHI Grant Number JP15H01836 and JP16H06443).

■ REFERENCES

- (1) Wang, G.; Tang, W.; Bidigare, R. R. Terpenoids As Therapeutic Drugs and Pharmaceutical Agents. In *Natural Products: Drug Discovery and Therapeutic Medicine*; Zhang, L., Demain, A. L., Eds.; Humana Press: Totowa, NJ, 2005; pp 197–227; DOI: 10.1007/978-1-59259-976-9_9.
- (2) Abe, I.; Rohmer, M.; Prestwich, G. D. *Chem. Rev.* **1993**, *93*, 2189–2206.
- (3) Wendt, K. U.; Schulz, G. E.; Corey, E. J.; Liu, D. R. *Angew. Chem., Int. Ed.* **2000**, *39*, 2812–2833.
- (4) Christianson, D. W. *Chem. Rev.* **2006**, *106*, 3412.
- (5) Abe, I. *Nat. Prod. Rep.* **2007**, *24*, 1311–1331.
- (6) Gao, Y.; Honzatko, R. B.; Peters, R. J. *Nat. Prod. Rep.* **2012**, *29*, 1153–1175.
- (7) Baunach, M.; Franke, J.; Hertweck, C. *Angew. Chem., Int. Ed.* **2015**, *54*, 2604–2626.
- (8) Wang, L.; Yang, B.; Lin, X.-P.; Zhou, X.-F.; Liu, Y. *Nat. Prod. Rep.* **2013**, *30*, 455–473.
- (9) Chiba, R.; Minami, A.; Gomi, K.; Oikawa, H. *Org. Lett.* **2013**, *15*, 594–597.
- (10) Matsuda, Y.; Mitsuhashi, T.; Quan, Z.; Abe, I. *Org. Lett.* **2015**, *17*, 4644–4647.
- (11) Ye, Y.; Minami, A.; Mandi, A.; Liu, C.; Taniguchi, T.; Kuzuyama, T.; Monde, K.; Gomi, K.; Oikawa, H. *J. Am. Chem. Soc.* **2015**, *137*, 11846–11853.
- (12) Qin, B.; Matsuda, Y.; Mori, T.; Okada, M.; Quan, Z.; Mitsuhashi, T.; Wakimoto, T.; Abe, I. *Angew. Chem., Int. Ed.* **2016**, *55*, 1658–1661.
- (13) Matsuda, Y.; Mitsuhashi, T.; Lee, S.; Hoshino, M.; Mori, T.; Okada, M.; Zhang, H.; Hayashi, F.; Fujita, M.; Abe, I. *Angew. Chem., Int. Ed.* **2016**, *55*, 5785–5788.
- (14) Toyomasu, T.; Tsukahara, M.; Kaneko, A.; Niida, R.; Mitsuhashi, W.; Dairi, T.; Kato, N.; Sassa, T. *Proc. Natl. Acad. Sci. U. S. A.* **2007**, *104*, 3084–3088.
- (15) Toyomasu, T.; Kaneko, A.; Tokiwano, T.; Kanno, Y.; Kanno, Y.; Niida, R.; Miura, S.; Nishioka, T.; Ikeda, C.; Mitsuhashi, W.; et al. *J. Org. Chem.* **2009**, *74*, 1541–1548.
- (16) Chen, M.; Chou, W. K.; Toyomasu, T.; Cane, D. E.; Christianson, D. W. *ACS Chem. Biol.* **2016**, *11*, 889–899.
- (17) Jin, F. J.; Maruyama, J.; Juvvadi, P. R.; Arioka, M.; Kitamoto, K. *FEMS Microbiol. Lett.* **2004**, *239*, 79–85.
- (18) Matsuda, Y.; Wakimoto, T.; Mori, T.; Awakawa, T.; Abe, I. *J. Am. Chem. Soc.* **2014**, *136*, 15326–15336.
- (19) Matsuda, Y.; Iwabuchi, T.; Wakimoto, T.; Awakawa, T.; Abe, I. *J. Am. Chem. Soc.* **2015**, *137*, 3393–3401.
- (20) Narita, K.; Chiba, R.; Minami, A.; Kodama, M.; Fujii, I.; Gomi, K.; Oikawa, H. *Org. Lett.* **2016**, *18*, 1980–1983.
- (21) Sugai, Y.; Ueno, Y.; Hayashi, K.-i.; Oogami, S.; Toyomasu, T.; Matsumoto, S.; Natsume, M.; Nozaki, H.; Kawaide, H. *J. Biol. Chem.* **2011**, *286*, 42840–42847.
- (22) Sugai, Y.; Miyazaki, S.; Mukai, S.; Yumoto, I.; Natsume, M.; Kawaide, H. *Biosci., Biotechnol., Biochem.* **2011**, *75*, 128–135.
- (23) Shimane, M.; Ueno, Y.; Morisaki, K.; Oogami, S.; Natsume, M.; Hayashi, K.-i.; Nozaki, H.; Kawaide, H. *Biochem. J.* **2014**, *462*, 539–546.
- (24) Jiang, J.; He, X.; Cane, D. E. *J. Am. Chem. Soc.* **2006**, *128*, 8128–8129.
- (25) Miller, D. J.; Gao, J.; Truhlar, D. G.; Young, N. J.; Gonzalez, V.; Allemann, R. K. *Org. Biomol. Chem.* **2008**, *6*, 2346–2354.

(26) Rabe, P.; Pahirulzaman, K. A.; Dickschat, J. S. *Angew. Chem., Int. Ed.* **2015**, *54*, 6041–6045.

(27) Rabe, P.; Rinkel, J.; Klapschinski, T. A.; Barra, L.; Dickschat, J. S. *Org. Biomol. Chem.* **2016**, *14*, 158–164.

(28) Rabe, P.; Janusko, A.; Goldfuss, B.; Dickschat, J. S. *ChemBioChem* **2016**, *17*, 146–149.

(29) Burkhardt, I.; Siemon, T.; Henrot, M.; Studt, L.; Rösler, S.; Tudzynski, B.; Christmann, M.; Dickschat, J. S. *Angew. Chem., Int. Ed.* **2016**, *55*, 8748–8751.

(30) Kaneda, M.; Takahashi, R.; Iitaka, Y.; Shibata, S. *Tetrahedron Lett.* **1972**, *13*, 4609–4611.

(31) Sugawara, H.; Kasuya, A.; Iitaka, Y.; Shibata, S. *Chem. Pharm. Bull.* **1991**, *39*, 3051–3054.

(32) Wang, Y.; Oberer, L.; Dreyfuss, M.; Sütterlin, C.; Riezman, H. *Helv. Chim. Acta* **1998**, *81*, 2031–2042.

(33) Sadler, I. H.; Simpson, T. J. *J. Chem. Soc., Chem. Commun.* **1989**, 1602–1604.

(34) Liu, Z.; Chen, Y.; Chen, S.; Liu, Y.; Lu, Y.; Chen, D.; Lin, Y.; Huang, X.; She, Z. *Org. Lett.* **2016**, *18*, 1406–1409.

(35) Kawahara, N.; Nozawa, M.; Flores, D.; Bonilla, P.; Sekita, S.; Satake, M.; Kawai, K.-i. *Chem. Pharm. Bull.* **1997**, *45*, 1717–1719.

(36) Lauer, U.; Anke, T.; Sheldrick, W.; Scherer, A.; Steglich, W. *J. Antibiot.* **1989**, *42*, 875–882.

(37) Fujii, T.; Yamaoka, H.; Gomi, K.; Kitamoto, K.; Kumaga, C. *Biosci., Biotechnol., Biochem.* **1995**, *59*, 1869–1874.

(38) Jin, F.; Maruyama, J.; Juvvadi, P.; Arioka, M.; Kitamoto, K. *Biosci., Biotechnol., Biochem.* **2004**, *68*, 656–662.

(39) Gomi, K.; Iimura, Y.; Hara, S. *Agric. Biol. Chem.* **1987**, *51*, 2549–2555.

(40) Frisch, M. J.; Trucks, G. W.; Schlegel, H. B.; Scuseria, G. E.; Robb, M. A.; Cheeseman, J. R.; Scalmani, G.; Barone, V.; Mennucci, B.; Petersson, G. A.; Nakatsuji, H.; Caricato, M.; Li, X.; Hratchian, H. P.; Izmaylov, A. F.; Bloino, J.; Zheng, G.; Sonnenberg, J. L.; Hada, M.; Ehara, M.; Toyota, K.; Fukuda, R.; Hasegawa, J.; Ishida, M.; Nakajima, T.; Honda, Y.; Kitao, O.; Nakai, H.; Vreven, T.; Montgomery, J. A., Jr.; Peralta, J. E.; Ogliaro, F.; Bearpark, M.; Heyd, J. J.; Brothers, E.; Kudin, K. N.; Staroverov, V. N.; Kobayashi, R.; Normand, J.; Raghavachari, K.; Rendell, A.; Burant, J. C.; Iyengar, S. S.; Tomasi, J.; Cossi, M.; Rega, N.; Millam, J. M.; Klene, M.; Knox, J. E.; Cross, J. B.; Bakken, V.; Adamo, C.; Jaramillo, J.; Gomperts, R.; Stratmann, R. E.; Yazyev, O.; Austin, A. J.; Cammi, R.; Pomelli, C.; Ochterski, J. W.; Martin, R. L.; Morokuma, K.; Zakrzewski, V. G.; Voth, G. A.; Salvador, P.; Dannenberg, J. J.; Dapprich, S.; Daniels, A. D.; Farkas, Ö.; Foresman, J. B.; Ortiz, J. V.; Cioslowski, J.; Fox, D. J. *Gaussian, Inc.*, Wallingford, CT, 2009.

(41) Halgren, T. A. *J. Comput. Chem.* **1996**, *17*, 490–519.